



## Chemical cleaning strategy of full-scale low-pressure reverse osmosis (LPRO) membrane process: case study

Hyojeon Kim<sup>a</sup>, Pattarasiri Fagkaew<sup>a</sup>, Kwangtaek Ahn<sup>b</sup>, Jaelim Lim<sup>c</sup>, Youngju Lee<sup>c</sup>, Seoktae Kang<sup>a,\*</sup>

<sup>a</sup>Department of Civil and Environmental Engineering, Korea Advanced Institute of Science and Technology, Daejeon, 34141, Korea, Tel. +82 42 350 3635; Fax: +82 42 350 3610; email: stkang@kaist.ac.kr (S. Kang)

<sup>b</sup>Water Supply Center, K-water Research Institute, Dangjin, 31710, Korea

<sup>c</sup>Water Resources Center, K-water Research Institute, Daejeon, 34045, Korea

Received 27 August 2017; Accepted 28 October 2017

### ABSTRACT

In this study, fouled reverse osmosis (RO) membranes from the full-scale low pressure reverse osmosis (LPRO) plant were autopsied in March (RO-M) and September (RO-S), and investigated before and after the chemical cleaning. The characteristics of residual matters on LPRO membrane surfaces were then determined via several analysis methods including excitation–emission matrix, molecular weight distribution, thermogravimetric analysis, and organic analyses. The foulants were predominantly composed of hydrophobic organic matters with dense structures on RO-S, while loose structure of CaSO<sub>4</sub> and BaSO<sub>4</sub> scaling dominantly covered membrane surfaces on RO-M. Interestingly, loose structure of scaling provided more significant growth of biofilm and subsequently higher organic mass per unit area on RO-M. The order of basic-acidic cleaning showed improved flux recovery (87%) than acidic-basic cleaning (79%) due to the dense structure of biofilm layer on RO-S. In case of RO-M, foulants were easily removed without regarding the order of chemical cleaning (higher than 93% of initial flux recovery) due to the loose structure of fouling layer. The results proposed that the membrane foulants might have seasonal differences, and the cleaning order of basic-acidic chemicals would provide higher flux recovery in the case of the fluctuation in influent quality.

*Keywords:* Reverse osmosis membrane; Autopsy; Case study; Cleaning strategy; Membrane characteristic

### 1. Introduction

Rapid urbanization and abnormal weather patterns over the past few decades caused the search of more sustainable water sources including not only river, lake, and ground water but also wastewater and seawater [1]. However, due to the increase in the use of various chemicals, it has been reported that emerging chemical contaminants are presented not only in wastewater but also in natural water [2]. These contaminants cannot be removed by conventional methods such as coagulation–flocculation and sand filtration, thus advanced treatment processes may also be required to

remove a wide range of components [3]. Based on these circumstances, pressure-driven membrane processes including nanofiltration and reverse osmosis (RO), have been widely used in water treatment and desalination applications due to their ability to remove most of undesirable compounds including salts and micropollutants [4–6].

One of the major limitation in the RO process is membrane fouling. The membrane fouling is affected by the operation conditions, feed water properties and membrane characteristics. Especially the feed water quality is closely related to the foulant characteristics such as dissolved organic substances, growth of microorganisms, inorganic compounds, and

\* Corresponding author.

particulate and colloidal matters [7–9]. To decrease fouling in water treatment using RO system, an accurate understanding of fouling, such as where fouling occurs, what type of fouling is dominant, the impact of feed water chemistry, and what operating conditions are more favorable, is necessary [8,9]. In order to identify the membrane properties, several methods such as molecular weight cut-off, bubble gas transport, water flux, and solute rejection evaluation, liquid equilibrium or thermoporometry and microscopic methods have been used. However, these conventional methods cannot directly describe to the solute permeation performances, which are the most significant features of membranes [3]. The fouled membrane autopsy of a pilot and full-scale conditions has been conducted in order to recognize the types and extent of fouling.

Chemical cleaning agents are usually applied to remove foulants that have accumulated on membrane surfaces, and classified as acid and base solution with additives such as surfactants and ethylenediaminetetraacetic acid [5]. However, chemical cleaning is typically performed as per manufacturer's guidelines, and it cannot guarantee the efficient cleaning due to the complexity of foulant characteristics. For this reason, a study on appropriate chemical cleaning strategies related to the fouling type should be conducted. Furthermore, it is necessary to make suitable cleaning strategy which can be physical, chemical or a combination of both based on the fouling properties [10].

In this study, properties of fouled RO membrane surfaces and deposited foulants were investigated by the autopsy of RO membrane module installed in commercial industrial LPRO membrane plant. Then, acidic and basic cleaning agents were applied in various order to correlate the properties of chemical cleaning agents with membrane flux recovery in order to provide better chemical cleaning strategies.

## 2. Material and methods

### 2.1. RO membrane and influent water quality

The RO membranes (ESPA, Hydranautics, Japan) were taken and autopsied from RO plant near D-city, Republic of Korea. The raw water is taken from a brackish water reservoir and pretreated by coagulation, flocculation and sedimentation processes. Then, the water is filtered through microfiltration (MF) membrane (Kolon, Republic of Korea; 0.05 mm pore), and used as the influent of RO process. The RO process is operated in two stages to supply pure water in industrial complex. Although the influent quality of the RO feed water have significantly changed over time, the average values during March and September (1 month prior to study) are summarized in Table 1.

### 2.2. Membrane autopsy and analysis of membrane surface

Fouled RO membranes were disassembled in March (RO-M) and September (RO-S) of 2016 when the operating pressure of RO system was increased to 150% of initial pressure. Both membrane samples were located at the first module in the first vessel of 1st stage. The module was autopsied as reported [6] and the fouled membrane coupons were stored at 4°C with 100% of humidity before the analysis. For the analysis of scanning electron microscopy (SEM,

Table 1

The influent water quality of RO process during March and September of 2015

Parameters	March (RO-M)	September (RO-S)
COD (mg/L)	15.5 ± 4.2	11.7 ± 3.1
SO <sub>4</sub> <sup>2-</sup> (mg/L)	151.1 ± 13.7	56.5 ± 8.5
Na (mg/L)	125.8 ± 11.5	41.0 ± 10.8
Ca (mg/L)	55.5 ± 5.2	28.0 ± 7.7
K (mg/L)	12.4 ± 1.3	7.5 ± 1.2
Mg (mg/L)	11.0 ± 6.4	4.8 ± 0.6
F (mg/L)	0.42 ± 0.14	0.53 ± 0.02
Mn (mg/L)	0.14 ± 0.08	0.02 ± 0.01

Carl Zeiss, Germany), energy dispersive X-ray spectroscopy (EDS; EDAX, USA) and Fourier transform infrared (FT-IR, PerkinElmer, USA), membrane coupons were cut and dried at 23°C overnight in the desiccator. The changes of hydrophobicity and surface free energy analyzed using contact angles (Phoenix, Korea) with three liquids: deionized water (DI), ethylene glycol (EG), and hexadecane (HD). The surface free energy was calculated using Lifshitz-van der Waals/Lewis acid-base (LW/AB) method [11].

### 2.3. Analysis of foulants on the membrane surface

In order to characterize the properties of organic and inorganic foulants on the RO membrane surface, foulants were separated using silicon knife, then dispersed in DI water for further analysis. The total solid mass and the content of organic matter were examined using a thermogravimetric analyzer (TGA) at 110°C–1,000°C with a heating rate of 10°C/min in atmosphere condition. The dissolved organic carbon (DOC) was measured using a total organic carbon analyzer (TOC-L, Shimadzu, Japan), and the fluorescence signal was measured by fluorescence spectrophotometer (RF-5301, Shimadzu, Japan) after samples were diluted to 1 mg-DOC/L.

### 2.4. Chemical cleaning procedure

To investigate the impact of the order during acidic and basic cleaning chemicals, fouled membranes were cleaned by commercial cleaning agents (Prime-Tech, Korea) with different orders (acid-base or base-acid). Briefly, fouled membrane coupons were soaked in 1.5% acid solution (pH 2.7) at 35°C for 12 h (Step A) with a vigorous stirring (300 rpm). In Step B, the fouled membrane was submerged in a 1.5% base solution (pH 11) for 12 h with a vigorous stirring. After each step, membrane samples were rinsed with DI to remove residual cleaning agents and membrane flux were measured using lab-scale testing units [5].

## 3. Results and discussions

### 3.1. Membrane surface characterizations

#### 3.1.1. SEM-EDS

The fouling structure from RO-S and RO-M is compared in Fig. 1, which presents the SEM micrographs of the top

layer of both membranes. Figs. 1(a) and (b) were taken from RO-S, and a dense and sticky fouling layer was found on the membrane surface. The EDS scanning revealed the fouling layer was mainly composed with carbon, oxygen, silica, aluminum, iron, and potassium. In contrast, crystals were found on the membrane surface from RO-M. EDS scanning of RO-M detected significant peaks of sulfur, aluminum, silicon, barium, and calcium, which indicated that barium sulfate and/or calcium sulfate scale was mainly related to the fouling layer [8,12,13]. The reason for the scale formation being more noticeable on RO-M sample is probably due to the feed water which contained higher concentrations of ion substances (Table 1).

### 3.1.2. FT-IR

In order to examine the changes of functional groups before and after the fouling, FT-IR spectra were measured as shown in Fig. 2. The specific peaks of polyamide around 1,487, 1,542, 1,584, and 1,650  $\text{cm}^{-1}$  were observed on the virgin membrane due to the amide I, amide II, and polysulfone support [14,15], while these peaks disappeared on RO-M and RO-S due to the formation of the fouling layer on the membrane surfaces. In addition, both fouled membrane samples exhibited additional signals between 1,150 and 1,250  $\text{cm}^{-1}$  related to the  $-\text{COOH}$  stretching from the carboxylic functional groups, which were probably due to organic matters originated from influent and/or microorganisms [5,16]. In addition, the major peak of the RO-S sample was at 3,300  $\text{cm}^{-1}$ , which corresponded to the N–H stretching from the amine groups. This peak had been acknowledged closely related to the build-up of biofouling layer [5,6,16,17]. Thus, by combining results from Figs. 1 and 2, it can be concluded that RO-S was mainly fouled with organic matters and/or biofilm, while the main

foulant on RO-M was inorganic precipitates such as calcium sulfate and barium sulfate.

### 3.1.3. Contact angle and surface free energy

The hydrophobicity of the membrane surfaces could be examined using the contact angle of water [18]. Furthermore, the wettability could be defined in terms of the surface free energy calculated from the measurement of contact angles with three liquid: water (DI), EG, and HD [19]. In Table 2, contact angles and results of surface free energy were summarized. As expected, the water contact angle of RO-S was higher than those of RO-M due to organic matters as

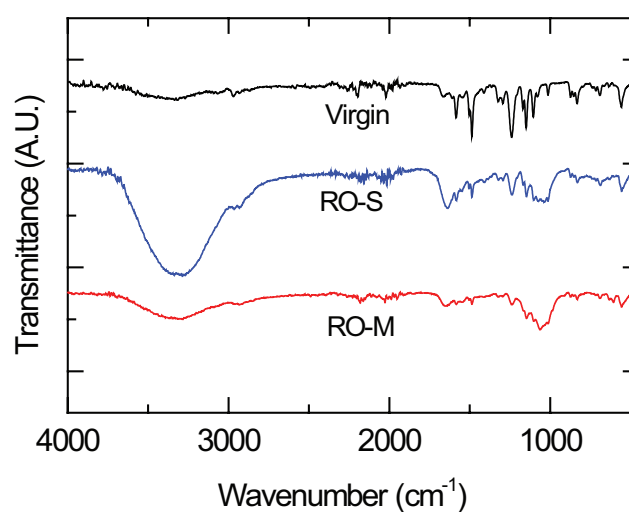


Fig. 2. FT-IR spectrum of virgin, RO-S and RO-M membrane surfaces.

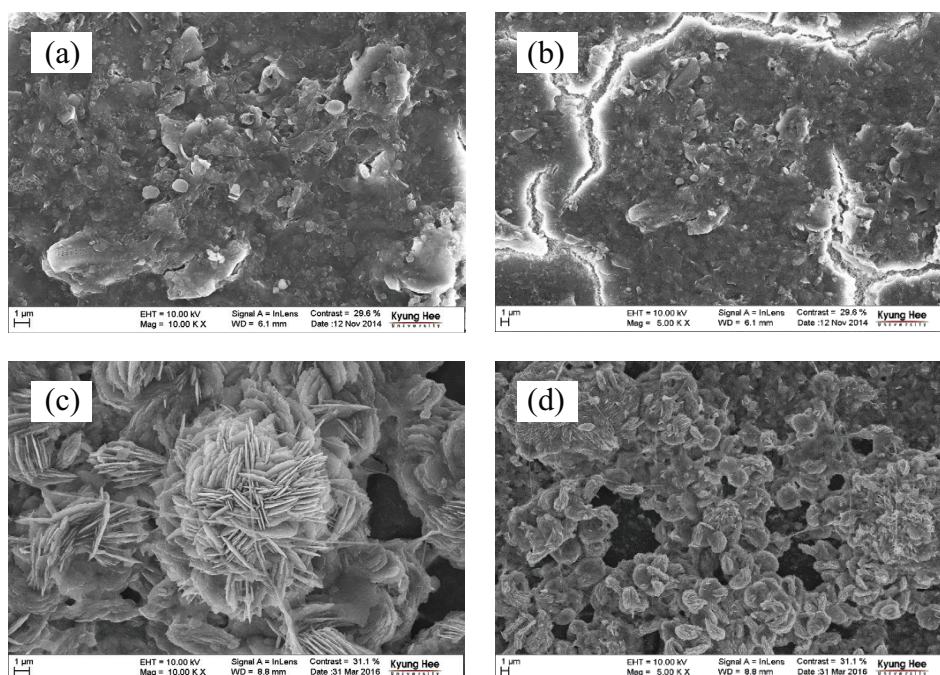


Fig. 1. SEM image of fouled membrane surfaces. (a) and (b) RO-S, and (c) and (d) RO-M.

indicated in Table 2. In the same manner, the surface free energy of the RO-S sample was lower than that of RO-M, which indicated hindered excess of water to the membrane surface. These results indicate that the RO-M sample surface was more hydrophilic and had higher wettability than the RO-S due to the inorganic scales on the membrane surface.

### 3.2. Thermal analysis

In the thermogravimetric analyses, it could be divided into three stages according to the temperature. In stage 1, the weight loss was attributed to the vaporization of the residual water and organic solvents under 100°C. In stage 2, the devolatilization happened which corresponded to the emission of volatile organic matters from various organic compounds under 350°C. Stage 3 was contributed to the weight loss due to the oxidization of the remaining volatile components. The differential thermogravimetric (DTG) and TGA curves obtained at a heating rate of 10°C/min are compared in Fig. 3. With increases in the temperature, a weight loss and a heat release were observed in the TGA and DTG curves, respectively. For the foulants acquired from RO-S sample,

Table 2  
Contact angles of three liquids and surface free energy (mJ/m<sup>2</sup>) of RO-M and RO-S membrane surfaces

	Contact angle (°)			$\gamma^{LW}$	$\gamma^+$	$\gamma^-$	$\gamma^{AB}$	$\gamma^{TOT}$
	DI	EG	HD					
RO-S	71.7	60.6	14.3	26.7	0.1	19.6	2.4	29.0
RO-M	32.4	31.4	12.3	26.9	0.8	58.1	13.4	40.3

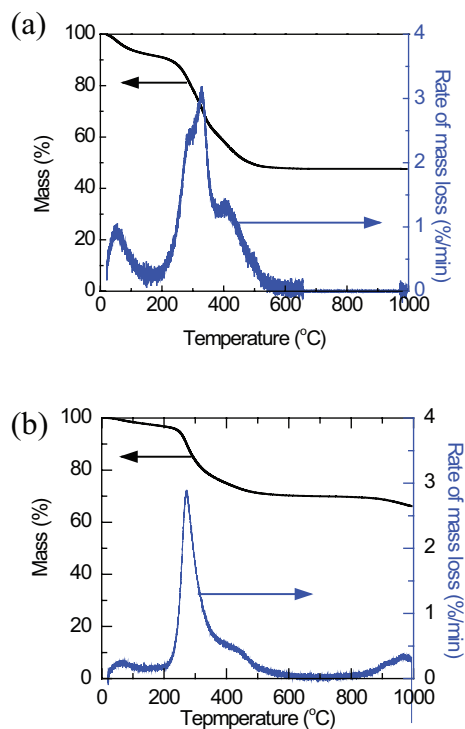


Fig. 3. The mass change and the rate of mass loss curves for foulants obtained from (a) RO-S, and (b) RO-M.

the largest weight loss occurred at approximately 327°C and the final mass loss which could be considered as organic content was 52.4%. For the RO-M sample, the largest weight loss occurred at approximately 271°C with a weight loss of only 33.8%. It implied that foulants on the RO-S sample were mainly complex organic matters, while majority of foulants on RO-M membrane surface is inorganic matters which could not be burned during TGA. Thus, from above results, organic fouling is dominant in RO-S and inorganic scaling is the main fouling mechanism on RO-M.

### 3.3. Characteristics of organic matters on fouled membrane surfaces

To investigate the characteristics of organic foulants, the foulants obtained on fouled membrane surfaces were sonicated and dissolved in DI water, then total suspended solids (TSS), chemical oxygen demand (COD), DOC, and specific UV absorption (SUVA) were measured as indicated in Table 3. Interestingly, the mass of pollutants per unit membrane area on the RO-S and RO-M samples were 176 and 959 mg/m<sup>2</sup>, respectively, while DOC of two samples were 41 and 81 mg/m<sup>2</sup>, respectively. Thus, it can be concluded that 23.3% of foulants on RO-S were carbon, but the carbon content in foulants from RO-M was only 8.4%. These results were in accordance with previous findings that RO-S was mainly fouled with organic and/or biofouling, while RO-M was fouled with scaling. SUVA data also represented that the organic matter on RO-S was more aromatic than RO-M, which was corresponded with their fouling mechanism.

In order to verify the origin of organic matters, excitation–emission matrix (EEM) were analyzed as shown in Fig. 4. The fluorescence spectrometry was categorized into four groups according to the previous report [20]: humic acid-like, fulvic acid-like, aromatic group, and soluble microbial by-product like (SMP). As fluorescence EEM spectra in Fig. 4, organic matters were mainly originated from microorganisms because EEM signals were only found in EEM category of aromatic groups and SMP. Thus, biofouling was the sole fouling mechanism in RO-S, and both scaling and biofouling were occurred on RO-M membrane surface. Moreover, the RO-M sample had a higher emission intensity than the RO-S sample due to the higher concentration of organic matters.

### 3.4. Chemical cleaning of fouled membranes

#### 3.4.1. Flux recovery

During the two steps (acidic and basic chemical cleaning) of cleaning procedures, many studies have shown that acidic chemicals (represented as A) are effective in removing

Table 3  
Characteristics of dissolvable component on fouled membranes

	RO-S	RO-M
TSS (mg/m <sup>2</sup> )	176	959
COD (mg/m <sup>2</sup> )	107.5	213.4
DOC (mg/m <sup>2</sup> )	41	81
SUVA (L/mg·m)	1.8	0.4

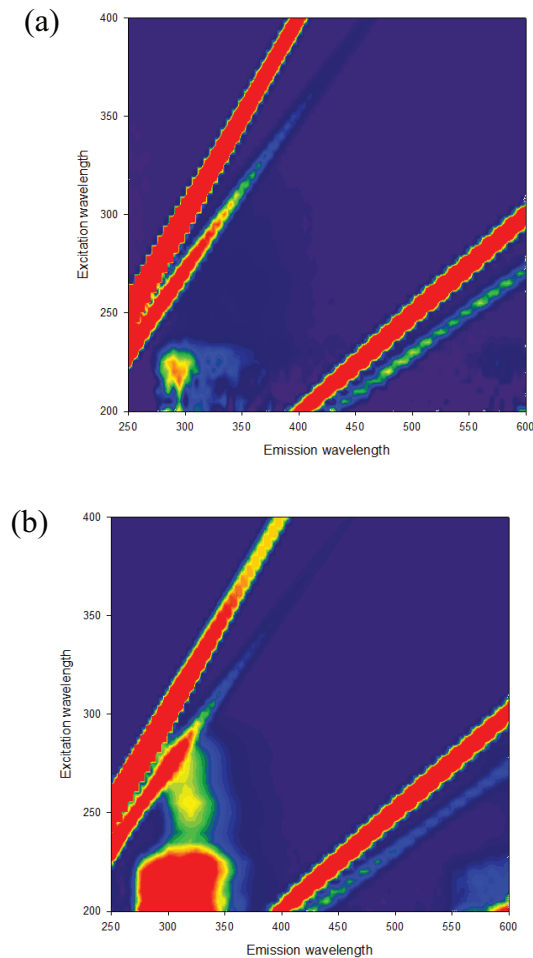


Fig. 4. The fluorescence EEM spectra of foulants obtained from (a) RO-S and (b) RO-M.

inorganic precipitates and loose the structure of organic fouling layer by dissolving cations such as  $\text{Ca}^{2+}$  or  $\text{Mg}^{2+}$ , while basic chemicals (represented as B) are effective in removing organic and bio-foulants by hydrolysis of organic matters [21,22]. As shown in Fig. 5(a), primary cleaning with acidic chemical showed 80% of initial flux recovery, and followed basic chemical cleaning resulted up to 87% of flux recovery compared with virgin membrane for the RO-S sample. Interestingly, in reverse order of chemical cleaning (B→A), basic chemical cleaning did not efficiently remove biofouling layer (i.e., 48% flux recovery), while flux was restored up to 79% after the acidic chemical cleaning. These findings highlighted that the dense structure of organic matters originated from microorganism should be first broken, so that the shear force induced by high cross-flow velocity should remove the biofouling layer. However, when we primarily applied basic chemical cleaning, only the top of biofouling layer seemed to be removed by hydrolytic reactions, thus the chemical could not affect the deeper region of biofouling layer. In contrast, the fouling layer of RO-M was mainly crystallized scaling with loose organic layer, and it induced effective permeation of basic cleaning chemicals into the fouling layer. As the result suggested, there were no noticeable differences between the two combinations of acidic and basic cleaning

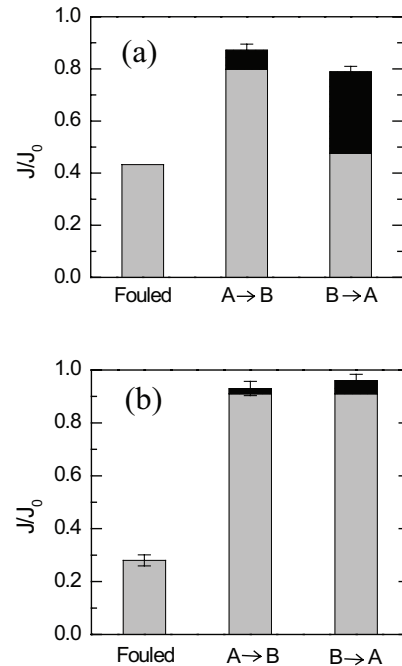


Fig. 5. The recovery of water flux ( $J/J_0$ ) according to the chemical order for (a) RO-S and (b) RO-M.

chemicals (Fig. 5(b)). Thus, regardless of fouling type (i.e., organic fouling or inorganic scaling), acidic chemical cleaning followed by basic chemical cleaning would provide better flux recovery than the other combination.

#### 3.4.2. Changes of surface morphology and free energy after chemical cleaning

As shown in Fig. 5, RO-M exhibited higher flux recovery (i.e., better chemical cleaning efficiency) than RO-S. SEM observations in Fig. 6 for each membrane surfaces also confirmed the better cleaning efficiency of RO-M. There were a lot of residual organic matters on RO-S even after chemical cleanings, while the characteristic rough structure of virgin membrane surfaces was observed in RO-M. As explained, it is due to the main constituents and their structure of fouling layers, that the densely structured organic layer hindered the intrusion of cleaning chemicals on RO-S, while the loosely formed crystal structure promoted the penetration of cleaning chemicals. These phenomena could be explained by surface free energy calculated from contact angle measurements between membranes and three liquids (DI, EG, and HD). As summarized in Table 4, RO-S exhibited significantly lower surface free energy, which denoted hindered diffusion of water molecules (thus cleaning chemicals) than virgin membrane due to the hydrophobic biofouling layer. However, surface free energy of RO-M was comparable with that of virgin membrane ( $40.3 \text{ mJ/m}^2$  vs.  $44.0 \text{ mJ/m}^2$ ), thus cleaning solution could easily access the inside of fouling layer.

After chemical cleanings, both membrane showed similar surface free energies with that of virgin membrane as shown in Table 4. Importantly, the value of surface free energies were directly proportional with flux recovery in Fig. 5. Consequently, the measurement of contact angles and

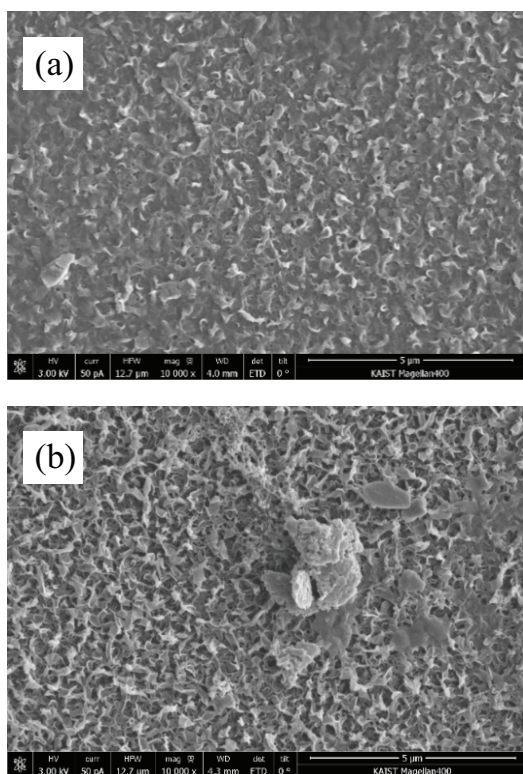


Fig. 6. SEM micrographs of chemically cleaned membrane with acidic chemicals followed by basic chemicals (A→B). (a) RO-S, (b) RO-M.

Table 4

Summary of surface free energy of RO-S and RO-M before and after chemical cleanings at different orders ( $\text{mJ}/\text{m}^2$ )

	Surface free energy ( $\text{mJ}/\text{m}^2$ )	
	RO-S	RO-M
Virgin	44.0	44.0
Fouled	29.0	40.3
A → B cleaned	36.5	45.6
B → A cleaned	40.3	46.8

calculation of surface free energies would be used for estimating chemical cleaning efficiencies.

#### 4. Conclusions

In this study, we autopsied and characterized the properties of fouling layer on RO membranes obtained from two seasons. The morphology of fouling layer, characteristics of foulants, and fouling type differed significantly according to the samples. Organic or biofouling layer exhibited more hydrophobic structure than inorganic scaling, while the mass of foulants per unit area was significantly high for inorganic scaling. During the chemical cleaning, the order of acidic and basic cleaning agents should be considered, and acidic chemical cleaning followed by basic chemical cleaning would provide higher flux recovery than the reverse order in both membrane samples.

#### Acknowledgments

This research was supported by a grant (code 171FIP-B088091-04) from Industrial Facilities & Infrastructure Research Program funded by Ministry of Land and by a grant (code 171FIP-B116952-02) from Plant Program funded by Ministry of Land, Infrastructure and Transport of Korean government.

#### References

- [1] C. Quist-Jensen, F. Macedonio, E. Drioli, Membrane technology for water production in agriculture: desalination and wastewater reuse, *Desalination*, 364 (2015) 17–32.
- [2] J. Radjenović, M. Petrović, F. Ventura, D. Barceló, Rejection of pharmaceuticals in nanofiltration and reverse osmosis membrane drinking water treatment, *Water Res.*, 42 (2008) 3601–3610.
- [3] B. Van der Bruggen, C. Vandecasteele, T. Van Gestel, W. Doyen, R. Leysen, A review of pressure-driven membrane processes in wastewater treatment and drinking water production, *Environ. Prog. Sustain. Energy*, 22 (2003) 46–56.
- [4] L. Malaeb, G.M. Ayoub, Reverse osmosis technology for water treatment: state of the art review, *Desalination*, 267 (2011) 1–8.
- [5] K. Ruengruehan, P. Fagkaew, G. Ahn, S. Kang, S.-O. Ko, Relating membrane surface properties and flux recovery during the chemical cleaning of forward osmosis membrane, *Desal. Wat. Treat.*, 57 (2016) 26621–26628.
- [6] F. Tang, H.-Y. Hu, L.-J. Sun, Q.-Y. Wu, Y.-M. Jiang, Y.-T. Guan, J.-J. Huang, Fouling of reverse osmosis membrane for municipal wastewater reclamation: autopsy results from a full-scale plant, *Desalination*, 349 (2014) 73–79.
- [7] H.L. Yang, C. Huang, J.R. Pan, Characteristics of RO foulants in a brackish water desalination plant, *Desalination*, 220 (2008) 353–358.
- [8] A. Antony, J.H. Low, S. Gray, A.E. Childress, P. Le-Clech, G. Leslie, Scale formation and control in high pressure membrane water treatment systems: a review, *J. Membr. Sci.*, 383 (2011) 1–16.
- [9] P. Xu, C. Bellona, J.E. Drewes, Fouling of nanofiltration and reverse osmosis membranes during municipal wastewater reclamation: membrane autopsy results from pilot-scale investigations, *J. Membr. Sci.*, 353 (2010) 111–121.
- [10] E. Antón, J.R. Álvarez, L. Palacio, P. Prádanos, A. Hernández, A. Pihlajamäki, S. Luque, Ageing of polyethersulfone ultrafiltration membranes under long-term exposures to alkaline and acidic cleaning solutions, *Chem. Eng. Sci.*, 134 (2015) 178–195.
- [11] T. Lin, Z. Lu, W. Chen, Interaction mechanisms and predictions on membrane fouling in an ultrafiltration system, using the XDLVO approach, *J. Membr. Sci.*, 461 (2014) 49–58.
- [12] N. Peña, S. Gallego, F. Del Vigo, S. Chesters, Evaluating impact of fouling on reverse osmosis membranes performance, *Desal. Wat. Treat.*, 51 (2013) 958–968.
- [13] C. Tzotzi, T. Pahiadaki, S. Yiantisios, A. Karabelas, N. Andritsos, A study of  $\text{CaCO}_3$  scale formation and inhibition in RO and NF membrane processes, *J. Membr. Sci.*, 296 (2007) 171–184.
- [14] V. Freger, J. Gilron, S. Belfer, TFC polyamide membranes modified by grafting of hydrophilic polymers: an FT-IR/AFM/TEM study, *J. Membr. Sci.*, 209 (2002) 283–292.
- [15] J.S. Louie, I. Pinnau, I. Ciobanu, K.P. Ishida, A. Ng, M. Reinhard, Effects of polyether–polyamide block copolymer coating on performance and fouling of reverse osmosis membranes, *J. Membr. Sci.*, 280 (2006) 762–770.
- [16] L.G. Benning, V. Phoenix, N. Yee, M. Tobin, Molecular characterization of cyanobacterial silicification using synchrotron infrared micro-spectroscopy, *Geochim. Cosmochim. Acta*, 68 (2004) 729–741.
- [17] L.B. Barber, J.A. Leenheer, T.I. Noyes, E.A. Stiles, Nature and transformation of dissolved organic matter in treatment wetlands, *Environ. Sci. Technol.*, 35 (2001) 4805–4816.

- [18] N. Lee, G. Amy, J.-P. Croue, H. Buisson, Identification and understanding of fouling in low-pressure membrane (MF/UF) filtration by natural organic matter (NOM), *Water Res.*, 38 (2004) 4511–4523.
- [19] G. Hurwitz, G.R. Guillen, E.M. Hoek, Probing polyamide membrane surface charge, zeta potential, wettability, and hydrophilicity with contact angle measurements, *J. Membr. Sci.*, 349 (2010) 349–357.
- [20] W. Chen, P. Westerhoff, J.A. Leenheer, K. Booksh, Fluorescence excitation-emission matrix regional integration to quantify spectra for dissolved organic matter, *Environ. Sci. Technol.*, 37 (2003) 5701–5710.
- [21] W.S. Ang, N.Y. Yip, A. Tiraferri, M. Elimelech, Chemical cleaning of RO membranes fouled by wastewater effluent: achieving higher efficiency with dual-step cleaning, *J. Membr. Sci.*, 382 (2011) 100–106.
- [22] S. Madaeni, S. Samieirad, Chemical cleaning of reverse osmosis membrane fouled by wastewater, *Desalination*, 257 (2010) 80–86.